

26. Z. Otwinowski and W. Minor, *Methods Enzymol.* **276**, 307 (1997).  
 27. J. Navaza, *Acta Crystallogr. D* **50**, 157 (1994).  
 28. A. T. Brünger et al., *Acta Crystallogr. D* **54**, 905 (1998).  
 29. T. A. Jones, J. Y. Zou, S. W. Cowan, M. Kjeldgaard, *Acta Crystallogr. A* **47**, 110 (1991).  
 30. S. C. Barker et al., *Biochemistry* **34**, 14843 (1995).  
 31. Z. Songyang et al., *Nature* **373**, 536 (1995).  
 32. S. Hubbard, L. Wei, L. Ellis, W. Hendrickson, *Nature* **372**, 746 (1994).  
 33. A. Wallace, R. Laskowski, J. Thornton, *Protein Eng.* **8**, 127 (1995).  
 34. We thank H. Viguier, L. Leighton, and N. Rodionova for technical assistance; H. Lewis, D. Jeruzalmi, and X. Chen for assistance with data collection and analysis; M. Huse, E. Vidal, and M. Young for valuable discussions; B. Mayer for kindly providing

mouse Abl cDNA; and K. Dorey, G. Superti-Furga, B. Brasher, and R. van Etten for communication of their unpublished results. T.S. acknowledges fellowship support from the Deutsche Forschungsgemeinschaft (Schi 524/1-1) and the Leukemia & Lymphoma Society. Protein coordinates are available from the Protein Data Bank (code 1fpu).

25 May 2000; accepted 25 July 2000

## Respiration and Parturition Affected by Conditional Overexpression of the Ca<sup>2+</sup>-Activated K<sup>+</sup> Channel Subunit, SK3

Chris T. Bond,<sup>1</sup> Rolf Sprengel,<sup>6</sup> John M. Bissonnette,<sup>2</sup> Walter A. Kaufmann,<sup>5</sup> David Pribnow,<sup>3</sup> Torben Neelands,<sup>1</sup> Thorsten Storck,<sup>6</sup> Manfred Baetscher,<sup>4</sup> Jasna Jerecic,<sup>6</sup> James Maylie,<sup>2</sup> Hans-Günther Knaus,<sup>5</sup> Peter H. Seeburg,<sup>6</sup> John P. Adelman<sup>1\*</sup>

In excitable cells, small-conductance Ca<sup>2+</sup>-activated potassium channels (SK channels) are responsible for the slow after-hyperpolarization that often follows an action potential. Three SK channel subunits have been molecularly characterized. The SK3 gene was targeted by homologous recombination for the insertion of a gene switch that permitted experimental regulation of SK3 expression while retaining normal SK3 promoter function. An absence of SK3 did not present overt phenotypic consequences. However, SK3 overexpression induced abnormal respiratory responses to hypoxia and compromised parturition. Both conditions were corrected by silencing the gene. The results implicate SK3 channels as potential therapeutic targets for disorders such as sleep apnea or sudden infant death syndrome and for regulating uterine contractions during labor.

SK channels are potassium-selective, voltage-independent, and activated by increases in the levels of intracellular Ca<sup>2+</sup>, such as what occurs during an action potential (1, 2). We have characterized three mammalian SK subunits (hSK1, rSK2, and rSK3) by molecular cloning. All three form SK channels with similar Ca<sup>2+</sup> sensitivity and gating kinetics; constitutive association of calmodulin accomplishes Ca<sup>2+</sup> gating with an intracellular domain of the channel  $\alpha$  subunits (3, 4). To investigate the physiological role of murine SK3, we site-specifically inserted a tetracycline-based genetic switch into the 5' untranslated region of the gene so that subunit expression could be abolished by dietary

doxycycline (dox) administration without interfering with the normal profile of SK3 expression (Fig. 1) (5).

SK3 mRNA levels were examined in brain tissue from wild-type (+/+), heterozygous (+/T), and homozygous (T/T) targeted mice that were without or with dox (0.5 mg/ml, for at least 5 days before being killed) in their drinking water. Total RNA from whole brains was used for Northern blot analysis and reverse transcriptase-polymerase chain reaction (RT-PCR) (Fig. 1). SK3 mRNA was readily detected from animals not treated with dox, but no hybridization signal was detected from dox-treated animals. Multiplex RT-PCR experiments for SK3 and  $\beta$ -actin (for cross-sample comparison), with equivalent amounts of cDNA from each animal, were analyzed during the linear range of amplification. Among wild-type animals, similar amounts of product were detected, and levels were not affected by dox. In heterozygous animals that were not treated with dox, expression from the two alleles was similar. After dox administration, levels derived from the wild-type allele were not significantly altered, but product derived from

the targeted allele was reduced to background levels. SK3 mRNA expression in homozygous targeted mice that were not administered dox was approximately three times that for either allele in heterozygous animals. Expression was undetectable after dox administration. To examine SK3 protein levels, we probed Western blots of membrane preparations from mouse brain with an SK3-specific antibody. SK3 protein was detected before but not after dox treatment. SK3 protein levels in the absence of dox were higher in SK3 T/T mice than in wild-type mice (Fig. 1) (6). Western blots for SK2 showed similar levels of protein in wild-type, T/T, or T/T with dox brain membrane preparations (7).

The regional distribution of SK3 protein in wild-type and SK3 T/T mice was investigated by immunohistochemistry in the brain (8, 9). Most immunoreactivity was associated with the neuropil; individual neuronal perikarya were only occasionally stained. The highest expression levels of SK3 protein were observed in the hippocampal formation, striatum, in subsets of neocortical neurons, thalamus, cerebellum, and brain stem. In particular, SK3 protein was detected in various neuronal populations of the medulla oblongata, which are thought to be involved in the processing of respiratory signals, e.g., the reticular formation and solitary tract nuclei (Fig. 2). For all brain regions investigated, the SK3 distribution profile remained unchanged in SK3 T/T mice when compared with wild-type animals. However, the absolute level of SK3 protein expression in SK3 T/T animals was higher. No SK3 immunoreactivity was detected in sections after dox treatment (Fig. 2). Together, these results demonstrate that, in mice homozygous for the conditional SK3 allele, SK3 expression in the brain is increased in relation to the wild type and expression can be abolished by dietary dox administration. The presence of the regulatory cassette in the exon encoding the 5' untranslated region does not alter the expression pattern of the SK3 gene.

SK3 is the only known SK subunit expressed in skeletal muscle where expression is highly induced by denervation and in primary cultured myotubes (10). To examine SK3 function in skeletal muscle from wild-type and SK3 T/T mice, we prepared myotube cultures in the presence or absence of dox (5  $\mu$ g/ml) in the media (11). After 6 days of culture, action potentials recorded from wild-type myotubes showed a prominent af-

<sup>1</sup>Vollum Institute, <sup>2</sup>Department of Obstetrics and Gynecology, <sup>3</sup>Department of Cell and Developmental Biology, <sup>4</sup>Department of Molecular and Medical Genetics, Oregon Health Sciences University, Portland, OR 97201, USA. <sup>5</sup>Institute of Biochemical Pharmacology, University of Innsbruck, A-6020 Innsbruck/Tyrol, Austria. <sup>6</sup>Department of Molecular Neuroscience, Max-Planck-Institute for Medical Research, D-69120 Heidelberg, Germany.

\*To whom correspondence should be addressed. E-mail: adelman@ohsu.edu

REPORTS

ter-hyperpolarization (Fig. 3) that was abolished by 30 nM apamin (7). The presence of dox in the media had no effect. In voltage clamp, step commands to depolarized potentials evoked sustained outward currents that were followed by outward tail currents upon repolarization. The sustained currents during the test pulse were partially blocked by apamin (30 nM), whereas the tail currents were completely suppressed (Fig. 3, left). The apparent voltage dependence of the SK current reflects the voltage dependence of Ca<sup>2+</sup> release from intracellular stores, consistent with skeletal muscle excitation-contraction coupling (12). Similar results were

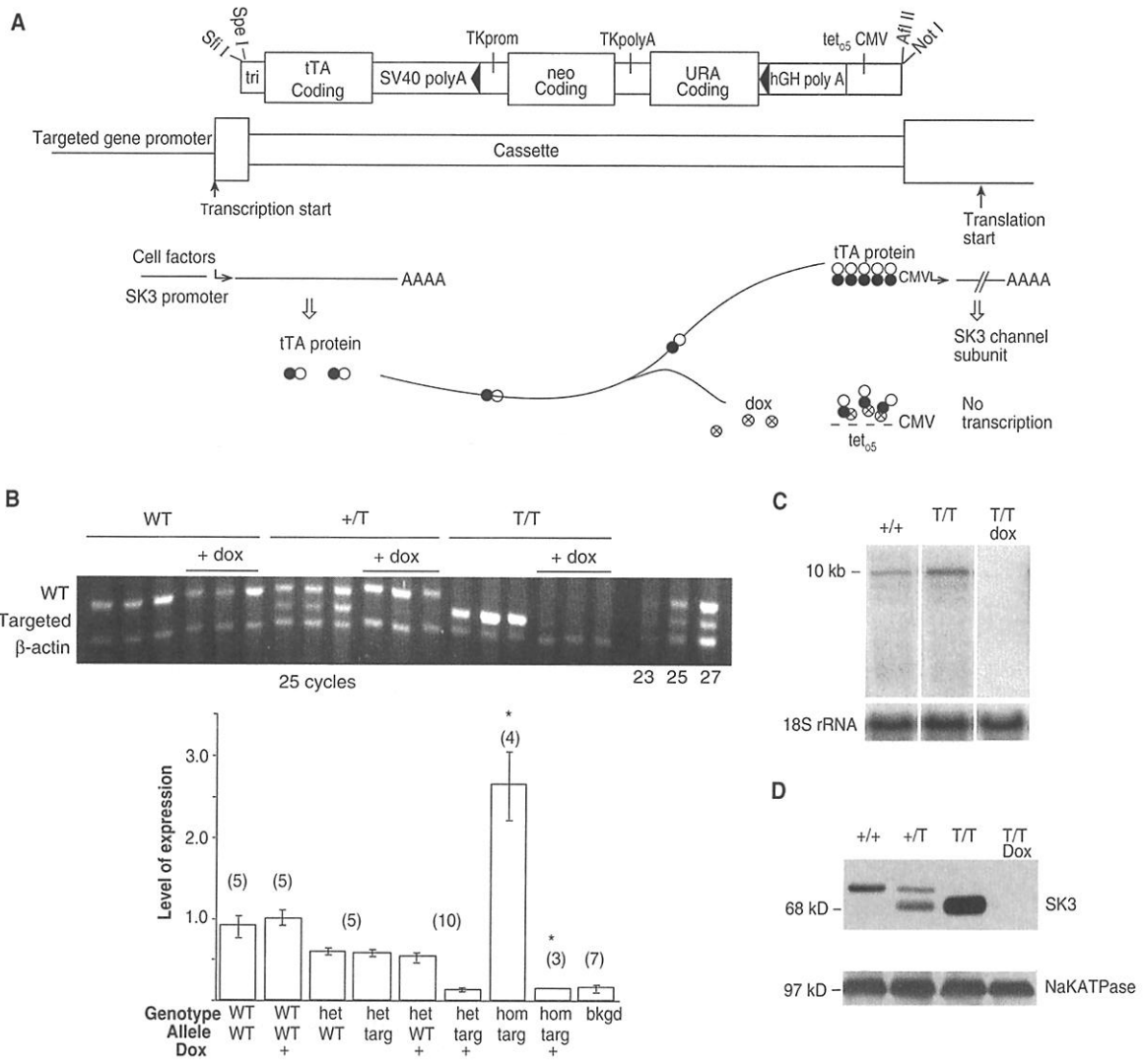
obtained for recordings from myotubes prepared from SK3 T/T mice cultured in the absence of dox (Fig. 3, middle column). The current density of the apamin-sensitive tail currents in wild-type and T/T myotubes cultured in the absence of dox was not different ( $3.7 \pm 0.3$  and  $4.0 \pm 0.8$  nA/pF, respectively). This may reflect maximal induction of SK3 expression in cultured myotubes, similar to the induction that occurs after denervation. In contrast, action potentials recorded from myotubes prepared from SK3 T/T mice and cultured in the presence of dox did not show after-hyperpolarization. In voltage clamp, apamin had no significant effect on either the

currents elicited during the voltage command or the tail currents (Fig. 3, right).

The administration of dox to pregnant females abolished SK3 expression in SK3 T/T neonatal mice but did not engender obvious developmental abnormalities. Similarly, no phenotypic consequences were observed from dox administration to homozygous SK3 T/T mice during postnatal or adult stages. As a result of the overexpression of SK3 in SK3 T/T mice that were not treated with dox (about threefold in the brain), two phenotypic consequences were observed.

We examined respiratory patterns under normal and hypoxic (8% O<sub>2</sub>) conditions (13).

**Fig. 1.** Regulation of SK3 gene expression in the brain. **(A)** Schematic representation of the regulatory cassette and the theory of the gene switch. The regulatory cassette is inserted into the 5' untranslated sequence and contains three functional modules. The 5' sequence encodes the binary tetracycline transactivator (tTA) protein (solid and open circles) (31) and is preceded by the adenovirus tripartite leader sequence that confers highly efficient translation initiation and followed by the polyadenylation/transcriptional termination sequence from SV40 (SV40 polyA). Second is the bacterial neomycin (G418) resistance gene driven by the herpes simplex virus thymidine kinase promoter and the yeast URA3 gene. These selectable markers are flanked by loxP sites (32) and are followed by the polyadenylation/transcription termination signal from the human growth hormone gene (hGH polyA) (33). The final module contains five copies of the tet operator fused to the minimal cytomegalovirus (tet<sub>5</sub> CMV) promoter. The native promoter drives expression of tTA that induces transcription of the structural gene from the tet<sub>5</sub> CMV promoter. Dox (crossed circles) interferes with the binding of tTA to its target sequence and abolishes transcription. **(B)** (top) A representative ethidium bromide-stained agarose gel of PCR products. Each lane is from an individual animal. The PCR was performed as a multiplex with β-actin for quantification; far right lanes show aliquots removed after the indicated number of PCR cycles, demonstrating that the PCR was analyzed during the linear phase of amplification. (bottom) Quantification of RT-PCR results. Two columns, WT (wild type) and targeted, are presented for heterozygous animals. Statistically



different groups are indicated by an asterisk ( $P < 0.05$ ; nonparametric analysis by Kruskal-Wallis one-way ANOVA). bkgd, background. **(C)** Northern blot of whole-brain total RNA (20 μg/lane) from wild-type and homozygous animals that were untreated or treated with dox (0.5 mg/ml) in drinking water for 4 days. The blot was probed with mSK3, stripped, and reprobed for 18S rRNA (bottom). **(D)** Western blots of mouse brain membrane preparations. The blot shown in the top panel was probed with an antibody to SK3. The duplicate blot shown in the bottom panel was probed with an antibody to Na<sup>+</sup>-K<sup>+</sup> ATPase. The difference in the size of the SK3 protein in the wild-type and SK3 T/T mice is due to the 40–amino acid deletion.

## REPORTS

**Fig. 2.** SK3 distribution in the mouse brain. Distribution of SK3 immunoreactivity (SK3-IR) at the level of the telencephalon/diencephalon, metencephalon, and myelencephalon in (**top**) homozygous targeted (T/T) and (**middle**) wild-type (WT) mice. SK3 immunoreactivity was detected in the Hi, Th, CPU, Cb, and Ve and in the dorsal, medial, and lateral regions of the myelencephalon (abbreviations are given below). (**bottom**) The left panel shows the Western blot of mouse brain membrane proteins (I, immune serum; PI, pre-immune serum; and Pep, competition with immunogenic peptide). The apparent molecular weight of SK3 is 79 kD. The middle two panels are high-power microphotographs of the dentate gyrus from T/T and wild-type mice (regions taken from top and middle panel, as depicted by the asterisks, respectively). The myelencephalic section (WT) was stained with preimmune serum, and the section from the dox-treated animal (dox) was stained with immune serum. Abbreviations are as follows: 3V, third ventricle; 4V, fourth ventricle; Amb, ambiguus nucleus; Amyg, amygdala; Cb, cerebellum; CPU, caudate putamen; D3V, dorsal third ventricle; g7, genu of facial nerve; Gi, gigantocellular nucleus; GL, granule cell layer; Hi, hippocampal formation; ic, internal capsule; IRT, intermediate reticular nucleus; LH, lateral hypothalamic area; MGP, medial globus pallidus; ML, molecular layer; mt, mammillothalamic tract; opt, optic tract; PcRt, parvocellular reticular nucleus; PL, polymorphic layer; Sol, solitary tract nuclei; Sp51, spinal trigeminal nucleus; Th, thalamus; and Ve, vestibular nuclei. Scale bars are as follows: telencephalon/diencephalon, 480  $\mu$ m; metencephalon, 315  $\mu$ m; myelencephalon, 220  $\mu$ m; high-power microphotographs in bottom panels, 75  $\mu$ m.

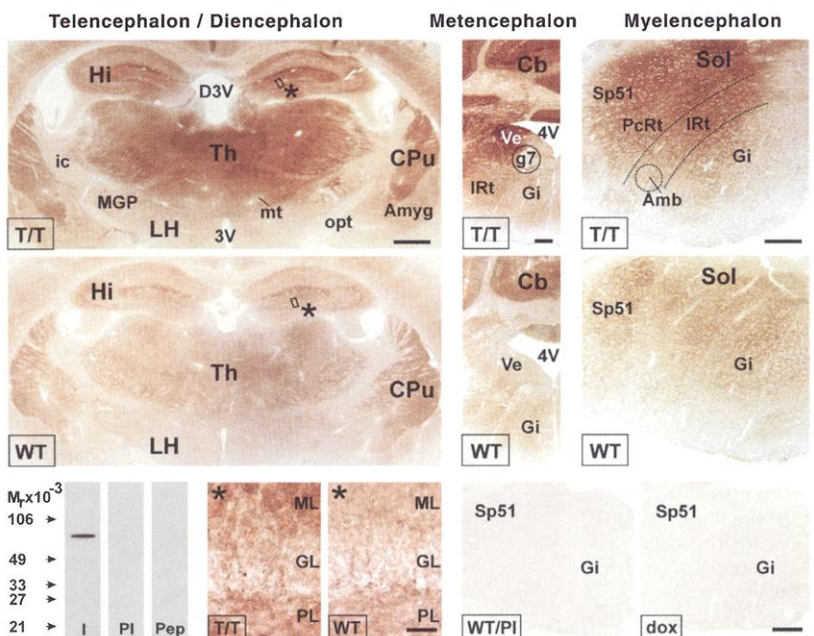
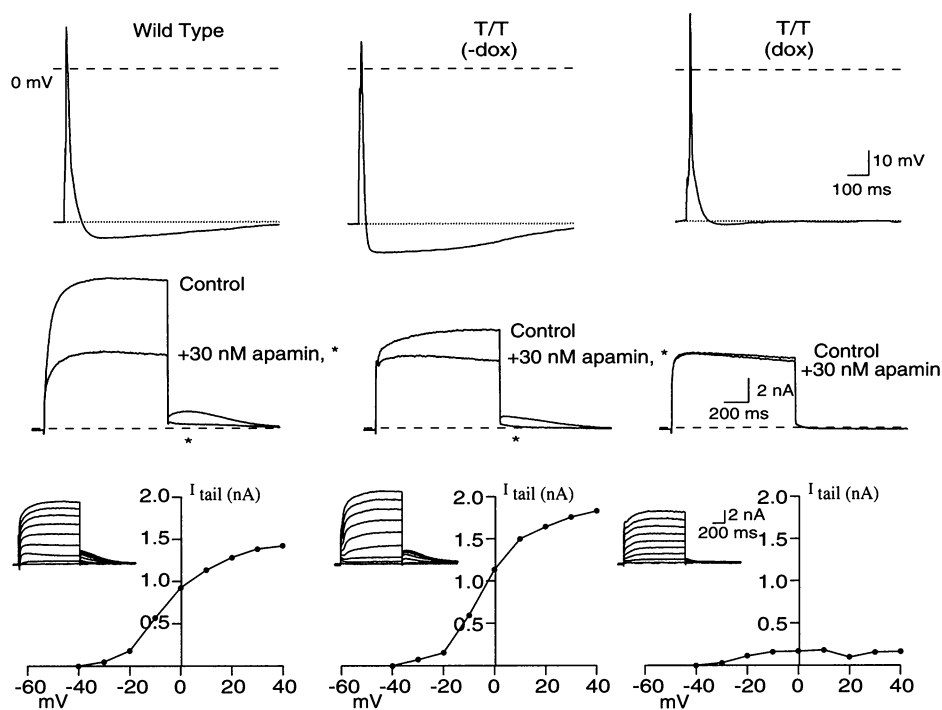


**Fig. 3.** Myotube electrophysiology. (**left**) Recordings from myotubes isolated from wild-type animals cultured with dox (5  $\mu$ g/ml). (**middle and right**) Recordings from myotubes isolated from SK3 T/T mice, cultured in the absence or presence of dox, respectively. Traces in each panel are from different cells. The top row of panels shows action potentials evoked by a 1-nA current injection for 3 to 10 ms. The dashed line represents 0 mV, and the dotted line is the resting membrane potential preceding the current injection. The middle row of panels shows current traces evoked by a 1-s voltage step to 40 mV from a holding potential of -50 mV and a return to -40 mV. The left and middle panels in this row illustrate the apamin-sensitive component in both the peak and tail currents (asterisks) for myotubes derived from either wild-type mice (with dox) or SK3 T/T mice (without dox). No significant apamin-sensitive current was seen in either the peak or tail currents from myotubes derived from SK3 T/T mice cultured in the presence of dox. The dashed line represents zero current. The bottom row of panels shows current-voltage relations of tail currents from the three different types of myotubes. From a holding potential of -50 mV, currents were evoked by depolarizing test potentials from -40 to 40 mV in 10-mV increments. The average outward tail current ( $I_{tail}$ ) measured 200 ms after return to -40 mV and is plotted as a function of the test potential. Myotubes from SK3 T/T mice cultured with dox showed minimal tail currents across the entire range of voltages tested (right panel in row). Insets show raw traces for each of the current-voltage plots.

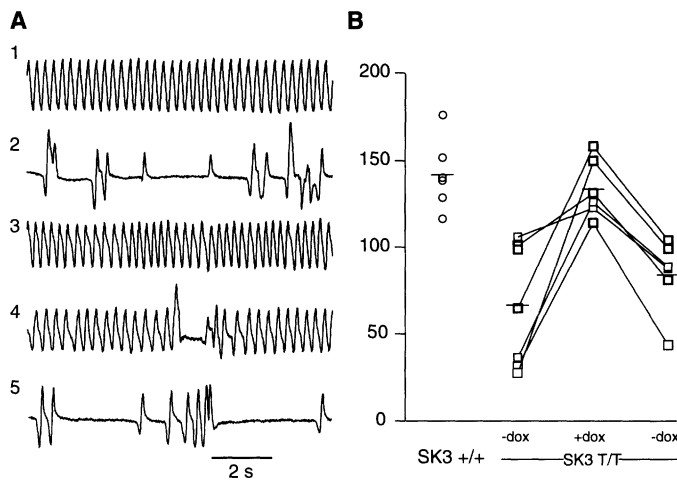


Respiratory timing in SK3 T/T mice ( $n = 7$ ) was not different from wild-type mice ( $n = 8$ ). In addition, the baseline respiratory pattern did not change significantly when SK3 T/T mice were treated with dox (500  $\mu$ g/ml for 2 weeks,  $n = 3$ , or 2 mg/ml for 6 days,  $n = 4$ ). Hypoxia in adult mammals is characterized by a sustained increase in breathing

rate (tachypnea) (14, 15). Upon hypoxic challenge, wild-type mice showed typical tachypnea that was sustained for 5 min. In SK3 T/T mice, there was an initial increase in respiratory frequency ( $122.0 \pm 8.5\%$  of control). The tachypnea lasted for only 30 to 45 s, and the frequency then declined to  $66.7 \pm 35.5\%$  of the baseline ( $P \ll 0.01$ ,

compared with SK3 wild-type mice). In three animals, apneic episodes in the second minute of hypoxia necessitated termination of the hypoxic challenge. In contrast, SK3 wild-type mice maintained an increase in frequency at  $142.9 \pm 20.6\%$  of the baseline in the second minute of hypoxia. SK3 T/T mice given dox (2 mg/ml in their drinking water

**Fig. 4.** Respiratory response to hypoxia. **(A)** Traces of respiratory pattern (inspiration is upward) in the second minute of hypoxia. Trace 1 is for the wild-type SK3<sup>+/+</sup> mouse, and traces 2 to 5 are for one individual SK3 T/T mouse studied serially as follows: trace 2, before dox administration; trace 3, after 6 days of dox administration (2 mg/ml in the drinking water); trace 4, 13 days after dox was discontinued; and trace 5, 20 days after dox was discontinued. **(B)** Average change in respiratory frequency during the second minute of exposure to hypoxia. Each symbol is the normalized average for an individual animal. Apneic episodes (expiratory time > 1.0 s) are not included in the determination of respiratory frequency. Horizontal lines indicate the mean for each group.



for 6 days) were restudied, and they showed a persistent increase of respiratory rate in hypoxia ( $134.6 \pm 17.0\%$  of control). These same mice, after being without dox for 20 to 35 days, were again unable to sustain a hyperpneic response to hypoxia (Fig. 4).

Crosses between SK3 T/T males and SK3 +/T females resulted in normal pregnancy and parturition. SK3 alleles were inherited in a Mendelian pattern, and homozygous pups were not obviously different from heterozygous littermates. Crosses between SK3 T/T mice showed that females demonstrated normal mating behavior, were fertile, and carried pups to term. However, in 7 out of 10 litters, delivery was protracted, and some of the pups did not survive; in four cases, females experienced distocia moribund, and mothers and pups did not survive. Subsequent autopsy revealed pups blocking the birth canal. No problems were encountered by wild-type or SK3 +/T females. In contrast, in 11 out of 11 cases, pregnant SK3 T/T mice that were administered dox (5  $\mu\text{g/ml}$ ) for 2 to 10 days before delivery underwent normal delivery. After delivery, dox administration was discontinued, and the pups developed normally. One homozygous female that had successfully delivered a viable litter while on dox was again bred after dox withdrawal. This time, parturition was unsuccessful, and mother and pups died. Western blot analysis detected high levels of SK3 protein in the uterus. To examine cell-type specificity, we crossed SK3 T/T mice with mice transgenic for the TA-driven lacZ gene (16).  $\beta$ -Galactosidase ( $\beta$ -Gal) activity was detected in the circular and longitudinal layers of uterine smooth muscle in offspring harboring both a targeted SK3 allele and the reporter  $\beta$ -Gal (7).

The conservation of three distinct SK genes with similar structures and biophysical

profiles and their distinct yet overlapping expression profiles indicate that they serve individual roles. Like other subfamilies of K<sup>+</sup> channels, SK channel subunits are structurally homologous and share basic gating and conduction properties. However, point mutations in K<sup>+</sup> channel genes underlie several inherited disorders, suggesting that each different K<sup>+</sup> channel subunit is essential for normal function (17–21). Further electrophysiological and behavioral examinations of mice lacking SK3 subunits will likely reveal less overt phenotypic consequences.

Overexpression of SK3 produced abnormal breathing patterns during hypoxic challenge and compromised parturition. These abnormalities may be caused by central mechanisms or reflect peripheral SK3 action only. SK3 protein is expressed in both populations of propriobulbar neurons within the Bötzing and pre-Bötzing complexes in the rostral ventrolateral medulla that are important for the generation and maintenance of respiratory pattern. An increased after-hyperpolarization, as might result from overexpression of SK3, could eliminate bursting patterns in inspiratory neurons (22). The inability to maintain enhanced respiratory rate is characterized by apneic episodes, suggesting that SK3 channels may be potential therapeutic targets for disorders such as sleep apnea or sudden infant death syndrome.

SK3 is prominently expressed in magnocellular neurons of the supraoptic nucleus and in many smooth muscles, including the uterus. Overexpression of SK3 in the magnocellular neurons might reduce hormone secretion, leading to problems during parturition. However, transgenic animals lacking oxytocin deliver successfully (23), suggesting that the problem resulting from SK3 overexpression may originate in the uterine smooth muscle, where an

exaggerated hyperpolarizing SK current might inhibit the development of a train of action potentials resulting in reduced contraction strength, compromising delivery. SK3 channels may also be involved in muscle hyperexcitability associated with myotonic dystrophy (DM) (24, 25). SK3 is the only known SK channel expressed in skeletal muscle, and direct apamin injection into affected muscle suppresses the myotonia (26). DM also results in several problems associated with pregnancy, including difficulties in expelling the fetus (27, 28), similar to the phenotype exhibited by female SK3 T/T mice.

The transgenic cassette employed in these studies permits acute regulation of the expression of a gene while leaving tissue-specific and developmental programming intact. Thus, dox administration reduced SK3 mRNA levels and protein levels below detection and reversed the pathological effects of SK3 overexpression. The effect on gene expression was reversible, as evidenced by the responses to hypoxic challenge before, during, and then after dox treatment. This strategy should be generally applicable and may overcome problems inherent to constitutive gene manipulations.

**References and Notes**

1. A. L. Blatz and K. L. Magleby, *Trends Neurosci.* **10**, 463 (1987).
2. M. Stocker, M. Krause, P. Pedarzi, *Proc. Natl. Acad. Sci. U.S.A.* **96**, 4662 (1999).
3. M. Köhler et al., *Science* **273**, 1709 (1996).
4. X.-M. Xia et al., *Nature* **395**, 503 (1998).
5. Mice harboring the regulatory cassette in the SK3 gene were developed as follows. The murine SK3 locus was isolated from a 129/SV genomic library (courtesy of M. Low, Vollum Institute). Nucleotide sequence analysis revealed an open reading frame (ORF) 5' to the initiator methionine used for heterologous expression studies of rat SK3 (3), extending the SK3 sequence by 174 amino acids to a methionine that is preceded by in-frame translational stop codons, similar to the human SK3 sequence (29). The regulatory cassette was inserted into SK3 genomic DNA by homologous recombination in a position 42 base pairs (bp) upstream of the most 5' methionine codon, and the targeting construct was electroporated into mouse J1 embryonic stem (ES) cells (gift of R. Jaenisch, Whitehead Institute, Boston, MA). Sequence analysis of the targeted SK3 allele showed that a deletion had eliminated 40 codons from the putative NH<sub>2</sub>-terminal coding region, deleting most of a predicted polymorphic polyglutamine stretch. Expression in *Xenopus* oocytes of SK3 mRNA containing the extended ORF, with or without the encoded polyglutamine repeat, did not alter current amplitudes, calcium sensitivity, or pharmacology. Injection of this ES cell clone into C57Bl/6 blastocysts gave rise to chimeric offspring, and the targeted allele was transmitted in crosses to C57Bl/6 females.
6. Ten micrograms of total RNA were reverse transcribed with random hexamers, and the cDNA was used in the PCR with Taq polymerase and SK3-specific primers (96°C for 30 s, 57°C for 30 s, and 72°C for 50 s, for 25 cycles). After 12 cycles, primers for  $\beta$ -actin were added, and cycling was continued. Aliquots were removed after 23 and 27 cycles to verify that amplification was in the linear range at 25 cycles. The SK3 5' PCR primer was directed to a sequence in the first exon, just 5' to the deletion on the targeted allele, and the 3' PCR primer was complementary to a sequence within the second exon. The 120-bp difference between RT-PCR products de-

rived from the mRNAs of wild-type and targeted SK3 alleles permitted quantification of the relative contribution by the two alleles. One-third of the PCR was prepared as a Southern blot, probed with a mixture of  $\beta$ -actin and SK3 oligonucleotides, and imaged on a PhosphorImager 4455I; signals were quantified with IP Lab Gel software (molecular Dynamics, Sunnyvale, CA). Data from individual animals were obtained in two to seven experiments, normalized to  $\beta$ -actin, standardized across experiments, and averaged to give one value per animal. These values were pooled according to genotype and drug treatment. For Northern blots, the total RNA was electrophoresed through a 1.4% agarose containing 1.0 M formaldehyde, blotted on nylon membranes, and probed for mouse SK3. A single SK3 mRNA, 10 kb, is detected in all mouse tissues, although two bands are detected in rat tissues (3, 70). Blots were stripped and re-probed for 18S rRNA. For Western blots, snap-frozen tissue was pulverized under liquid nitrogen, hand-dounced in ice-cold sucrose (320 mM) with mammalian protease inhibitor cocktail (Sigma), and microfuged at 10,000g for 10 min at 4°C; the supernatant was centrifuged at 100,000g at 4°C for 60 min. The membrane pellet was resuspended in sucrose with mammalian protease inhibitor cocktail and sonicated for 10 s. Western blots (20  $\mu$ g) were prepared and probed with antibody to SK3 (1:1000) or antibody to Na<sup>+</sup>- and K<sup>+</sup>-dependent adenosine triphosphatase (Na<sup>+</sup>,K<sup>+</sup>-ATPase) (1:50,000) (gift of S. Luchenko). Following secondary antibody (goat antirabbit immunoglobulin G—horseradish peroxidase), immunoreactivity was detected with Super Signal West Pico Chemiluminescent Substrate and X-Omat Blue XB-1 film.

7. C. T. Bond, J. Maylie, J. P. Adelman, unpublished observation.

8. A polyclonal antiserum directed against SK3 protein was raised in rabbits using the immunogenic peptide ADTLRQQQQLLAFVEAR, synthesized on a Lys<sup>9</sup> core linked to a solid-phase peptide synthesis support (A, Ala; D, Asp; E, Glu; F, Phe; L, Leu; Q, Gln; R, Arg; T, Thr; and V, Val). Antibodies were used for all immunohistochemistry experiments and the Western blot presented in Fig. 2. SK3 immunoreactivity was localized with an avidin-biotin peroxidase method with 40- $\mu$ m free-floating cryostat sections. Antibody was applied at a dilution of 1:80,000.

9. W. A. Kaufmann *et al.*, *Eur. J. Neurosci.* **10**, 1084 (1998).

10. D. Pribnow *et al.*, *Muscle Nerve* **22**, 742 (1999).

11. Cultured myotubes were prepared from the hindlimb muscles of postnatal day 2 mice (30). Whole-cell patch clamp recordings were performed on multinucleated myotubes 6 to 9 days after plating. Culture dishes were perfused with oxygenated Tyrode solution (140 mM NaCl, 5 mM KCl, 1 mM MgCl<sub>2</sub>, 10 mM dextrose, 10 mM Hepes, and 1.8 mM CaCl<sub>2</sub>) with pH of 7.35. Patch electrodes (2 to 4 megohms) were filled with internal solution (105 mM K<sup>+</sup> aspartate, 10 mM NaCl, 10 mM Hepes, 40 mM KCl, 1 mM MgCl<sub>2</sub>, 0.05 mM EGTA, and 5 mM Mg-adenosine 5'-triphosphate) with pH of 7.10. Nearly all cells visibly contracted during voltage steps or ramps. Statistical significance was determined post hoc by analysis of variance (ANOVA) and Bonferroni tests.

12. T. Tanabe, K. G. Beam, B. A. Adams, T. Niidome, S. Numa, *Nature* **346**, 569 (1990).

13. Baseline respiratory pattern and the response to hypoxia (8% oxygen for 5 min at 30°C) were measured in a body plethysmograph. Individual unanesthetized animals were placed in a 65-ml chamber with their head exposed. A pneumotachograph was connected to the chamber and to a differential pressure transducer. The analog signal from the transducer was amplified, converted to digital, displayed on a monitor, and stored to disk by computer for later analysis. Results are expressed as a percentage of the baseline respiratory rate determined during 5 min before the hypoxia. In separate studies of respiratory timing, inspiratory time, expiratory time, respiratory cycle duration, and the fraction of the respiratory cycle duration occupied by the inspiratory time were determined by analyzing 50 consecutive breaths for a representative period of 15 min in air. Data are expressed as mean  $\pm$  SD, and differences between groups were examined with one-way ANOVA followed by the Newman-Keuls test.

14. J. P. Mortola, in *Tissue Oxygen Deprivation*, G. G. Haddad and G. Lister, Eds. (Dekker, New York, 1996), pp. 433–477.

15. D. Gozal *et al.*, *Am. J. Respir. Crit. Care Med.* **155**, 1755 (1997).

16. J. Jerecic *et al.*, *Ann. N.Y. Acad. Sci.* **868**, 27 (1999).

17. D. L. Browne *et al.*, *Nature Genet.* **8**, 136 (1994).

18. J. P. Adelman, C. T. Bond, M. Pessia, J. Maylie, *Neuron* **15**, 1449 (1995).

19. S. M. Zuberi *et al.*, *Brain* **122**, 817 (1999).

20. B. C. Schroeder, C. Kubisch, V. Stein, T. J. Jentsch, *Nature* **396**, 687 (1998).

21. C. Biervert *et al.*, *Science* **279**, 403 (1998).

22. J. M. Ramirez and D. W. Richter, *Curr. Opin. Neurobiol.* **6**, 817 (1996).

23. K. Nishimori *et al.*, *Proc. Natl. Acad. Sci. U.S.A.* **93**, 11699 (1996).

24. J. F. Renaud *et al.*, *Nature* **319**, 678 (1986).

25. D. Pribnow and J. P. Adelman, *Curr. Res. Ion Channel Modulators* **3**, 221 (1999).

26. M. I. Behrens, P. Jalil, A. Serani, F. Vergara, O. Alvarez, *Muscle Nerve* **17**, 1264 (1994).

27. P. Dufour *et al.*, *Eur. J. Obstet. Gynecol. Reprod. Biol.* **72**, 159 (1997).

28. S. Rudnik-Schoneborn, G. A. Nicholson, G. Morgan, D. Rohrig, K. Zerres, *Am. J. Med. Genet.* **80**, 314 (1998).

29. K. G. Chandry *et al.*, *Mol. Psychiatry* **3**, 32 (1998).

30. A. L. Blatz and K. L. Magleby, *Nature* **323**, 718 (1986).

31. P. A. Furth *et al.*, *Proc. Natl. Acad. Sci. U.S.A.* **91**, 9302 (1994).

32. N. Sternberg and D. Hamilton, *J. Mol. Biol.* **150**, 467 (1981).

33. E. Y. Chen *et al.*, *Genomics* **4**, 479 (1989).

34. We thank H. Bujard for graciously providing elements of the tTA system. This work was supported by grants from the NIH, the Muscular Dystrophy Association, the Human Frontiers of Science Program, and ICAgen (to J.P.A. and J.M.) and by the Volkswagen Foundation and the Bristol-Myers Squibb Foundation (to P.H.S.).

4 January 2000; accepted 21 July 2000

## Interhemispheric Asymmetries of the Modular Structure in Human Temporal Cortex

Ralf A. W. Galuske,<sup>1\*</sup> Wolfgang Schlote,<sup>2</sup> Hansjürgen Bratzke,<sup>3</sup> Wolf Singer<sup>1</sup>

Language-relevant processing of auditory signals is lateralized and involves the posterior part of Brodmann area 22. We found that the functional lateralization in this area was accompanied by interhemispheric differences in the organization of the intrinsic microcircuitry. Neuronal tract tracing revealed a modular network of long-range intrinsic connections linking regularly spaced clusters of neurons. Although the cluster diameter was similar in both hemispheres, their spacing was about 20 percent larger in the left hemisphere. Assuming similar relations between functional and anatomical architecture as in visual cortex, the present data suggest that more functionally distinct columnar systems are included per surface unit in the left than in the right area 22.

Neuropsychological, electrophysiological, and noninvasive imaging studies indicate that language comprehension and production are accompanied by activation of certain cortical areas. Several of these areas are activated only unilaterally in the dominant hemisphere (1, 2). One of the regions exhibiting robust

unilateral activation during processing of language-related signals is located in the posterior part of the first temporal gyrus and the posterior temporal plane (Fig. 1A) (3–6). This region corresponds to a discrete cytoarchitectonical entity, the posterior part of area 22 in the Brodmann classification (7), or to

Table 1. Interpatch distances and patch sizes in area 22.

Patient	Distance (left/right)	n	p*	Size (left/right)	n	p*
M1	1450 $\mu$ m	10	0.0114	856 $\mu$ m	10	0.7
	1236 $\mu$ m	16		844 $\mu$ m	26	
M2	1432 $\mu$ m	22	<0.0001	689 $\mu$ m	24	0.015
	1099 $\mu$ m	27		616 $\mu$ m	36	
M3	1463 $\mu$ m	20	0.0402	728 $\mu$ m	24	0.49
	1234 $\mu$ m	23		707 $\mu$ m	23	
M4	1544 $\mu$ m	43	0.0016	746 $\mu$ m	58	0.64
	1303 $\mu$ m	34		734 $\mu$ m	42	
M8	1630 $\mu$ m	28	0.0203	823 $\mu$ m	28	0.39
	1464 $\mu$ m	30		802 $\mu$ m	27	
M9	1149 $\mu$ m	45	0.0294	572 $\mu$ m	48	0.41
	1022 $\mu$ m	23		558 $\mu$ m	26	
M11	1370 $\mu$ m	44	0.0341	589 $\mu$ m	47	0.0797
	1207 $\mu$ m	19		640 $\mu$ m	19	

\*P values arising from Mann-Whitney U test.